Electrical characterization of individual metal-coated polymer spheres used in isotropic conductive adhesives

Hoang-Vu Nguyen,[1] Jianying He,[2] Tore Helland,[3] Helge Kristiansen,[4] Knut E. Aasmundtveit[1]

[1]Department of Micro and Nano Systems Technology, University College of Southeast Norway, Raveien 215, Borre 3184, Norway
[2]NTNU Nanomechanical Lab, Norwegian University of Science and Technology (NTNU), Richard Birkelands Vei 1A, Trondheim 7491, Norway
[3]Mosaic Solutions AS, Dragonveien 54, Skjetten 2013, Norway
[4]Conpart AS, Dragonveien 54, Skjetten 2013, Norway
Correspondence to: H.-V. Nguyen (E-mail: hoang.v.nguyen@hbv.no)

ABSTRACT: Isotropic conductive adhesives (ICAs) filled with metal-coated polymer spheres (MPS) have been proposed to improve the mechanical reliability compared to conventional ICAs filled with silver flakes. The electrical properties of MPS play an important role in the electrical performance of macroscopic MPS-based ICAs. This article deals with the electrical characterization of individual MPS using a nanoindentation-based flat punch method, in which the resistance and the deformation of single MPS were monitored simultaneously. Four groups of silver-coated polymer spheres (AgPS) with identical polymer cores but different silver coating thicknesses were tested. The resistance of AgPS decreases gradually with increasing deformation degree of particles, and increases when the deformation of particles is reduced. In addition, the resistance of individual AgPS is dependent on the physical properties of the silver coating, such as thickness, uniformity, and porosity. The thicker the silver coating is, the lower and more stable the resistance of AgPS is. © 2016 Wiley Periodicals, Inc. J. Appl. Polym. Sci. **2016**, *133*, 43764.

INTRODUCTION

Isotropic conductive adhesives (ICAs) have been commercially available as an alternative to solder interconnects in electronic packaging for decades. An ICA consists of a polymeric adhesive matrix filled with electrically conductive particles. The mechanical strength of the ICA joint comes from the matrix, while the particles provide electrical conductivity. Traditional ICA compounds are loaded with 25–30 vol % (up to 80 wt %) of solid silver (Ag) particles (typically in flake-form) to ensure the required electrical conductivity.[1] As the thermo-mechanical properties of Ag, such as the coefficient of thermal expansion (CTE) and the elastic modulus, are very different from those of the adhesive matrix,[2] a large fraction of Ag particles in a conventional ICA causes high local stress induced in the bulk of the material. This is believed to be the main source for the poor mechanical performance of the conventional ICAs in environmental stress tests, such as drop (impact) tests and thermo-mechanical cycling.[1,3] Poor mechanical performance in various demanding conditions is an obstacle to widespread industrial adoption of the ICA technology.[3]

A novel idea for improving the flexibility, and hence the mechanical reliability, of the ICAs is to replace the solid Ag particles with metal-coated polymer spheres (MPS).[4,5] Compared to the solid Ag particles, the thermo-mechanical properties, such as the CTE and the elastic modulus, of the MPS are much better matched to those of the adhesive matrix. Thereby, stress concentrations at the interfaces between the MPS and the adhesive, and hence the stress induced in the bulk of the ICAs, can be reduced. Besides that, MPS in the adhesive matrix can also behave as the component for mechanical energy absorption. Consequently, the ICA resistance to dynamic mechanical loading (typically vibration and shock) can be improved. Another advantage of using MPS to replace the solid Ag particles is that the amount of metal needed in the ICAs is considerably reduced. This introduces the possibility to use noble metals at relatively low cost.

One concern when loading an adhesive with MPS has been that the electrical percolation threshold (the minimum particle fraction where satisfactory conductivity of the ICA first occurs) will increase compared to ICAs loaded with traditional flake-like

particles.[6] A higher particle concentration may critically impact the viscosity, and hence limit the processability of MPS-based ICAs. In addition, a higher particle concentration, that is, a lower volume fraction of the adhesive matrix, may result in an MPS-based ICA with low mechanical strength. In previous studies,[7–9] we have characterized the rheological properties and the mechanical properties of an adhesive filled with 45 vol % Ag-coated monodisperse polymer spheres (AgPS), representing a complete MPS-based ICA. The rheological behavior of the ICA showed a high potential for processing capabilities. Furthermore, the ICA with 45 vol % AgPS exhibited an improved mechanical performance over conventional Ag-filled ICAs.

Another concern with MPS-based ICAs has been the electrical conductivity of the materials, compared to conventional Ag-filled ICAs. Replacing solid Ag particles with MPS significantly reduces the amount of metal in the ICA, and hence may influence the electrical conductivity of ICAs based on MPS. In previous studies of the electrical properties of ICAs filled with AgPS,[10,11] our characterization showed a percolation threshold in the range of 25–35 vol %. Importantly, the electrical conductivity of the adhesive containing 45–50 vol % of AgPS was close to that of a commercial Ag-filled ICA, but with a dramatically reduced Ag content.

The electrical conductivity of MPS-based ICAs relies on several factors including particle concentration, conducting mechanisms between particles in the adhesive matrix (particle–particle contact and/or tunnelling effect), and especially the bulk conductivity of particles. The present work deals with the conductivity of particles in terms of electrical characterization for individual MPS. Four groups of AgPS with identical polymer core but different Ag coating thickness were tested to study effects of the coating on the electrical conductivity of particles. The electrical characterization of individual AgPS was performed using a nanoindentation-based flat punch method, in which electrical resistance and deformation of individual particles were monitored simultaneously. The measurement results were compared with a theoretical model for bulk resistance of individual particles to examine factors with important impact on resistance of AgPS. The results in this work are useful to develop a theoretical model to predict the electrical resistance of ICAs filled with AgPS.

EXPERIMENTAL

Four groups of AgPS were tested in the present study. All particles consist of an identical Ø30 μm methacrylate-based polymer core coated with an Ag layer. Particles of the four groups have the Ag coating thickness of 0.10, 0.15, 0.20, 0.25 μm, and are denoted A010, A015, A020, A025, respectively. Scanning electron microscopy (SEM) micrographs of particles in the four groups are shown in Figure 1. All particles were supplied by Conpart AS (Norway), and were used as received.

The characterization of AgPS was performed using a nanoindentation-based flat punch method. The method has recently been developed for measuring mechanical and electrical performance of individual micron-sized MPS.[12–15] A nanoindentation testing system (TriboIndenter® 900 from Hysitron Inc.) was employed to conduct the characterization for

individual AgPS. A flat punch of 75 μm in diameter was specifically designed. The punch is made of tungsten carbide with 10% cobalt (WC-Co). Test substrates were made from a silicon (Si) wafer with a sputtered gold (Au) thin film of 0.2 μm. The Au-coated Si wafer was supplied by Acreo AB (Sweden). The flat punch and the Au-coated substrates were also connected with wires to measure electrical resistance of AgPS using the four-point probe method. The four-point resistance measurements were carried out using a Keithley 2602 source meter. Figure 2(a) illustrates the experimental setup for the electrical measurements of individual particles.

Prior to the indentation tests for each group of particles, a tiny amount of dry particles were dispersed onto an Au-coated Si substrate (one new substrate for each group of particles). Using the integrated optical microscope of the TriboIndenter, individual particles with sufficient distance to the closest neighbor were identified for the indentation tests. Prior to each test, the flat punch was cleaned to remove external impurities. Each test was performed with a virgin particle. All tests were performed in air and at room temperature (23 °C). A force controlled mode was operated for the indentation tests of all particles, in which the applied force follows a predefined profile. The loading profile of all tests is shown in Figure 2(b). A maximum load of 8 mN was selected due to the limit of the transducer, and the fact that AgPS was expected to have a limited deformation in ICAs. During the indentation test for each particle, the electrical resistance measurement was conducted in a specific period, as illustrated in Figure 2(b), to prevent tested particle from being destroyed due to sparks that occur when the flat punch contacts the particle. After each indentation test, force, deformation, and resistance were recorded as function of time for each particle.

RESULTS

Mechanical Response

Force-deformation curves for the four groups of AgPS are shown in Figure 3. With the same loading profile, the mechanical response of all tested particles is similar. The deformation of a particle increases with increasing force applied, and decreases when the applying force releases. Hysteresis is also observed from the force-deformation curves, indicating viscoelastic deformation of the particles. No fracture points are observed for all tested particles under the 8 mN peak load. The force-deformation curves of A010, A020, and A025 particles [Figure 3(a,c,d)] are less scattered, compared to that of A015 particles.

Electrical Resistance Measurement Results

Figure 4 shows an example of resistance measurement data for one single AgPS particle. Due to low measured signals and a short acquisition time, the signal-to-noise ratio was low for the resistance measurement. Therefore, raw measurement data were influenced by noise. As resistance measurement results were to be correlated with mechanical deformation data for each particle, the measured resistance and deformation must have the same sampling rate. However, due to the availability of equipment, the resistance data and the force-deformation data were recorded with different sampling rates. Therefore, the resistance measurement data were fitted using a nonparametric fitting tool in MATLAB to extract resistance data with the same sampling
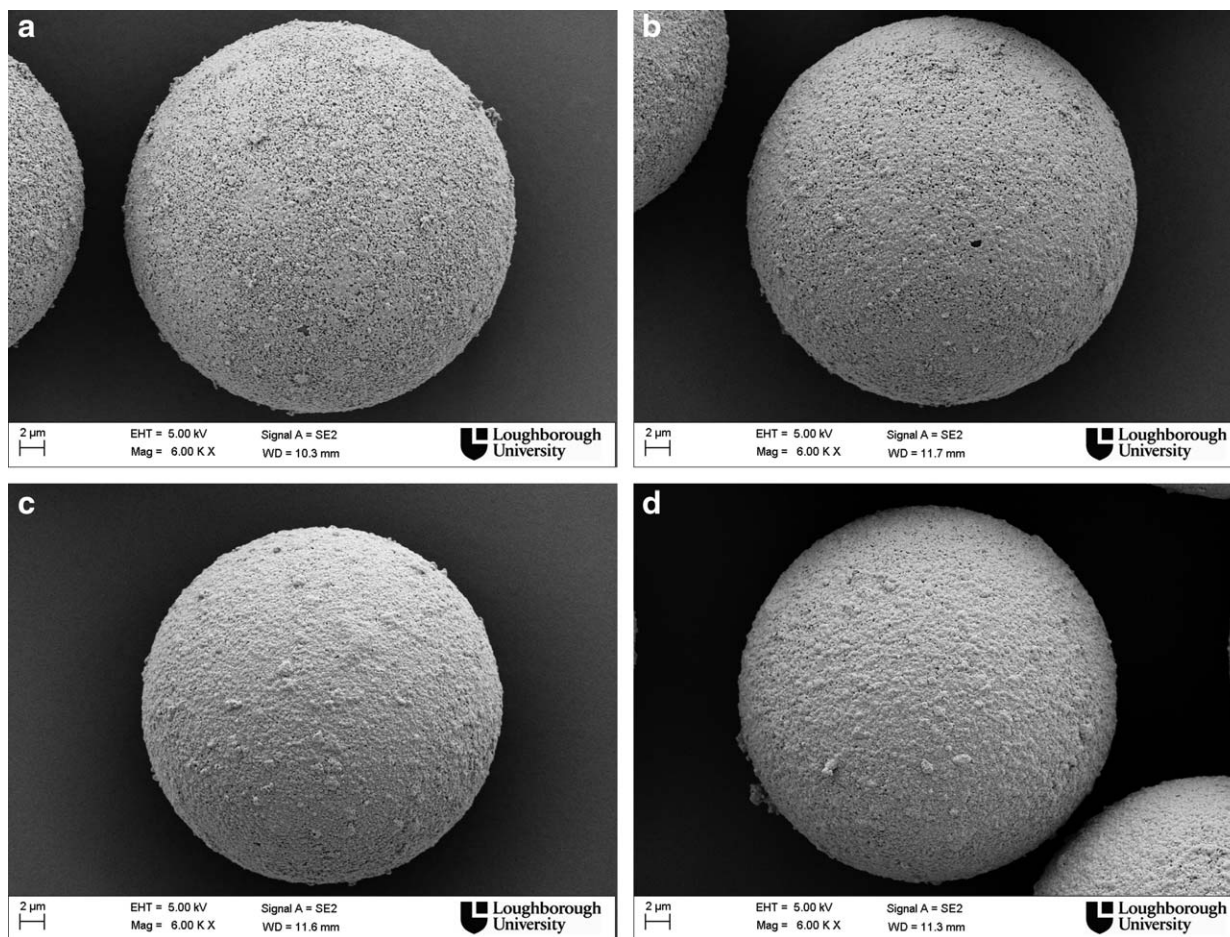
Figure 1. SEM images of particles consisting of Ø30 μm polymer spheres coated with (a) 0.10 μm thick (A010), (b) 0.15 μm thick (A015), (c) 0.20 μm thick (A020), and (d) 0.25 μm thick (A025) Ag coating.

rate as the deformation data. For all tested particles, the root mean squared deviation of the data fitting is in the range of 0.025–0.030 Ω. Fit data are relevant representations for resistance measurement results, with root mean squared deviation representing measurement accuracy.

Figure 5 shows an example of electrical resistance and corresponding deformation as function of time for an individual AgPS. Figure 6 shows the resistance vs. deformation for the four groups of AgPS tested. In general, the resistance of individual particles decreases gradually with increasing deformation degree of particles, and increases when the deformation of particles is reduced during the unloading of applied force. Among the four groups of particles, A010 particles with the thinnest Ag coating show relatively high and scattered resistance, compared to particles with thicker Ag coating (A015, A020, and A025). It is evident that the thicker the Ag coating is, the lower and less scattered the electrical resistance is.

DISCUSSION

Mechanical Response of Individual AgPS

The mechanical responses under applied force of the four groups of AgPS were compared, as shown in Figure 7. The typical force-deformation curve for each group was selected as the median one among those shown in Figure 3. In general, the particles of four groups A010, A015, A020, and A025, with identical polymer core but different Ag-coating thickness, exhibit similar mechanical response. This implies no significant effect of the coating thickness on the mechanical properties of particles. With a maximum loading force of 8 mN, the maximum deformation of AgPS is around 1.5–2 μm, which is only about 5–7% of the particle diameter ($\sim$30 μm). At such low deformation degrees, a small difference in mechanical properties of AgPS with relatively thin Ag coating (less than 2% of the polymer core radius) should be expected. This observation is based on a previous study of Helland,[16] in which the effect of coating thickness on the mechanical properties of nickel-coated polymer spheres was small when the coating thickness was less than 3% of the polymer core radius. As Ag is much softer than nickel,[2] the same behavior is expected for AgPS characterized in the present study.

The particles of all four groups characterized in this study have an identical polymer core but different Ag-coating thickness. Whereas the indentation force-deformation curves are repeatable for the tested particles in groups A010, A020, and A025, a somewhat larger scatter in the measured curves is observed for A015 particles. This may be attributed to the sample
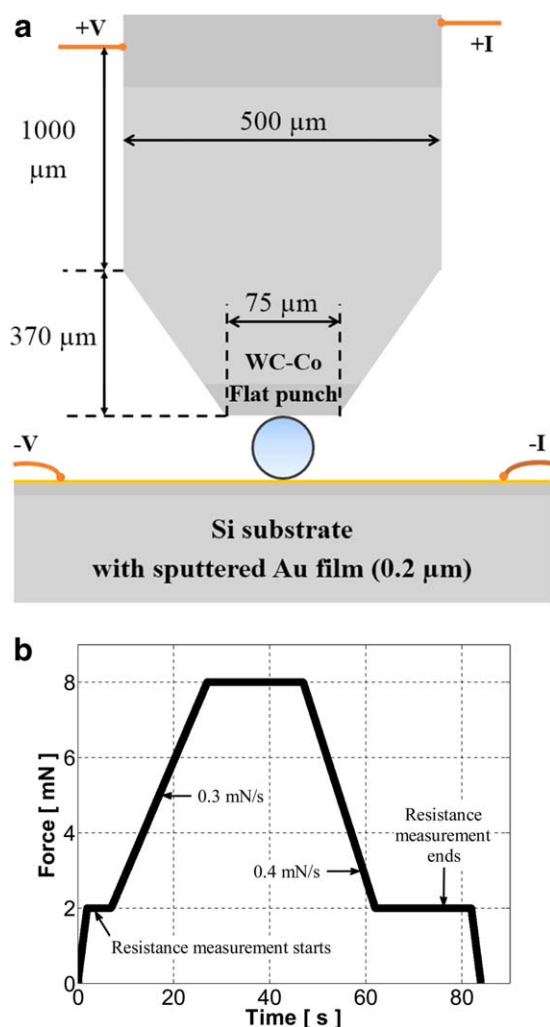
Figure 2. Experimental setup for the electrical measurements of individual particles using a nanoindentation-based flat punch test (a), and loading profile of all indentation tests (b). The drawing for the experimental setup is not to the scale. The period of the electrical measurements is indicated in Figure 2(b). [Color figure can be viewed in the online issue, which is available at wileyonlinelibrary.com.]

preparation of the substrate used for the measurements of A015 particles.

In the present study, electrical resistance measurements were performed while individual particles were under deformation. The current applied during the resistance measurements may influence the mechanical response of the particles due to heating. This topic, however, is beyond the scope of the present study and will be addressed in further studies.

Electrical Resistance Measurement Results of Individual AgPS Effect of Ag Coating on Resistance. Among the four groups of AgPS tested, A010 particles exhibit highest resistance with relatively large scattering. While the highest resistance of A010 particles is evidently due to the thinnest Ag coating, the large scattering of measured resistance is attributed to the inhomogeneous coating thickness of particles in the same group, which is related to the plating process. The effect of inhomogeneous

coating on particle resistance would relatively be larger for groups of particles with thinner Ag coating (e.g., A010) than for groups with thicker Ag coating.

Factors Contributing to Measurement Results of Individual AgPS. As can be seen from the experimental setup [Figure 2(a)], the measurement result of an individual AgPS includes bulk resistance of the particle, resistance of the flat punch, and interfacial contact resistances between the particle and the punch as well as between the particle and the Au-coated substrate. In this section, we assess the contribution of the flat punch resistance and the interfacial contact resistances to the measurement results.

Contribution of flat punch resistance. The resistance of the flat punch is considered between the location where the $(V+)$ wire is connected and the flat surface of the punch [Figure 2(a)]. This resistance is regarded as the resistance of a cone in series with a cylinder, which are made of WC-Co with a resistivity of about 200 n$\Omega \cdot$m.[17] Based on the geometries of the cone and the cylinder shown in Figure 2(a), the resistance of the flat punch contributing to the measurement results is calculated about 4 mΩ. This resistance value is negligible, compared to the measurement results for individual AgPS (in the range of several hundreds of mΩ).

Contribution of interfacial contact resistance. The interfacial contact resistance between an AgPS and a flat plate (i.e., the punch or the Au-coated substrate) consists of constriction resistance and tunnelling resistance. The constriction resistance is induced by the narrowing of conduction path due to small contact area between the particle and the flat plate. The tunnelling resistance is related to any insulating film which may separate the two contact surfaces. In the present study, the tunnelling resistances are not considered due to metal-to-metal contacts between the AgPS particle and the two surfaces of the punch and the Au-coated substrate. Therefore, the interfacial contact resistances are mainly governed by the constriction resistances.

The constriction resistance between two contacting bodies can be estimated using a theoretical model of Holm for a single contact spot.[18–20] The model was derived by assuming that the contact area is circular and continuous (i.e., perfectly smooth contact surfaces), and that the contact radius is much smaller than the geometrical dimensions of the contacting bodies. The formula of Holm model for the constriction resistance between two contacting bodies is given in the following equation.[18]

$$R_c = (\rho_1 + \rho_2)/(4 \cdot a) \quad (1)$$

where R_c is the constriction resistance; ρ_1 and ρ_2 are the electrical resistivity of the two metals in contact; and a is the contact radius. For small deformations of an elastic sphere against rigid plates, the relation between the contact radius (i.e., contact area) and the deformation of the sphere (i.e., applied force) can be estimated by using Hertz's theory of elastic contact.[21–23] The principal assumptions of the Hertz contact theory are that the load applied between contacting bodies is normal; the deformation is small and purely elastic; the contact surfaces are perfectly smooth; and that there is no adhesion and friction between
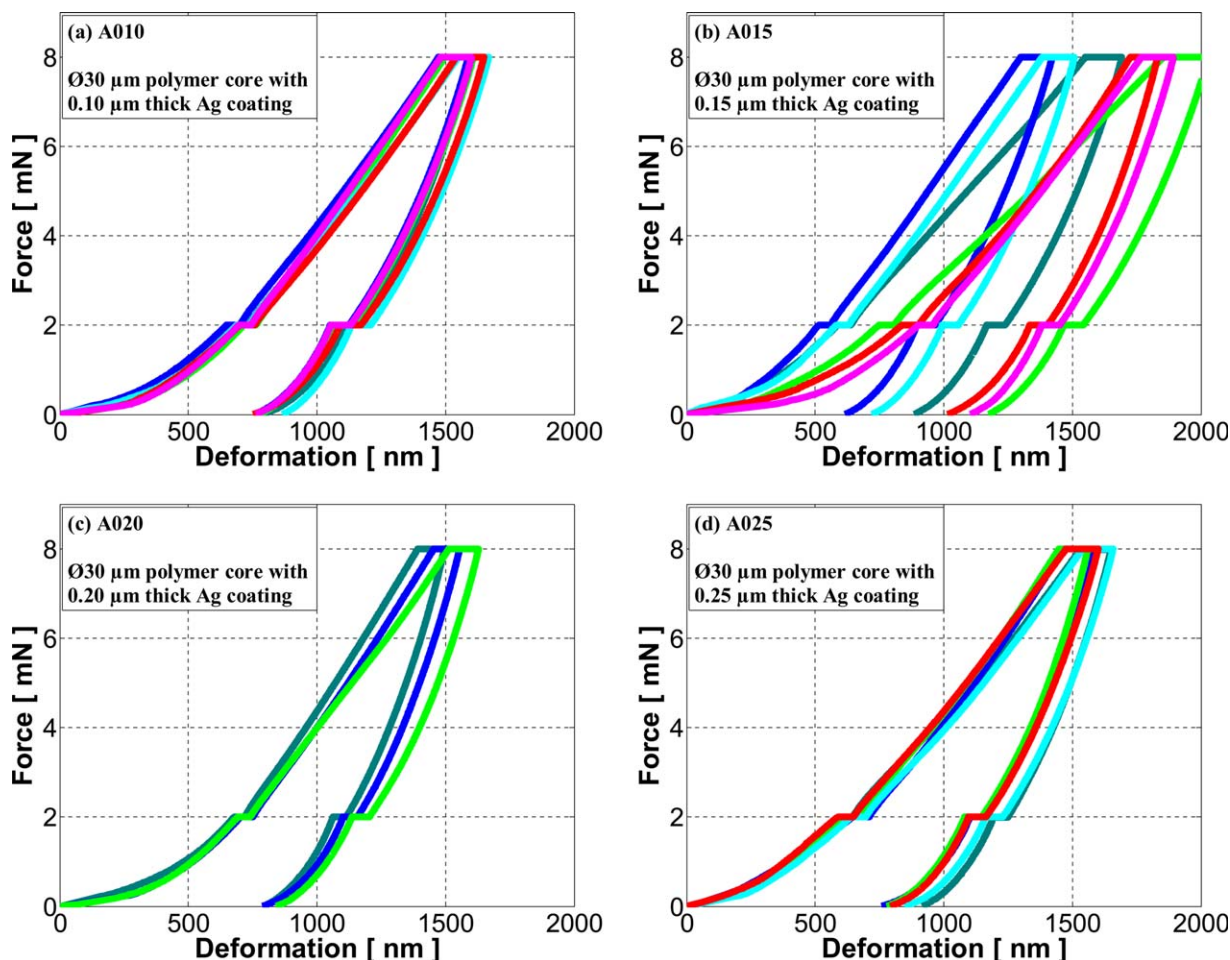
Figure 3. Indentation force-deformation curves for the four groups of AgPS. Each curve in a graph presents measurement result of an individual particle from the corresponding group. The plateaus in each force-deformation curve are corresponding to the holding segments on the loading profile, where applied force is held constant at 2 mN, 8 mN, and then 2 mN [Figure 2(b)]. The loading rate from 2mN to 8 mN and the unloading rate from 8 mN to 2 mN are 0.3 mN/s and 0.4 mN/s, respectively. [Color figure can be viewed in the online issue, which is available at wileyonlinelibrary.com.]

contact surfaces. The relation between the contact radius and the total deformation of a particle is given in the following equation.[21,23]

$$a=\sqrt{r \cdot (D/2)} \qquad (2)$$

where a is the contact radius; r is the original radius of the particle; and D is the total deformation of the particle.

The theoretical models of Holm and Hertz have been commonly used in previous studies of electrical conduction of
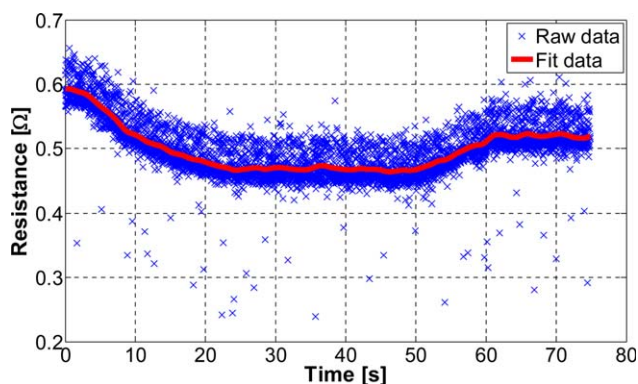

Figure 4. Example of resistance measurement result for an individual AgPS from group A020; raw data vs. fit data. The root mean squared deviation of the data fitting is about 0.026 Ω. [Color figure can be viewed in the online issue, which is available at wileyonlinelibrary.com.]
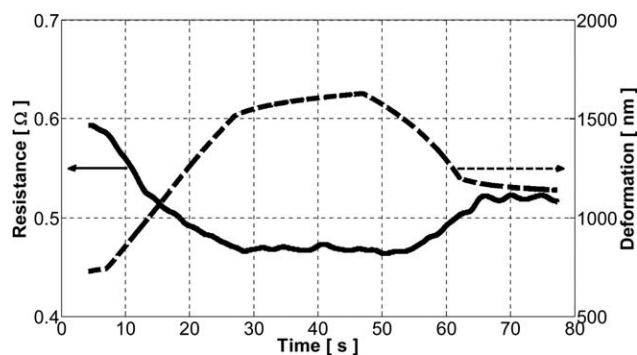

Figure 5. Example of electrical resistance and corresponding deformation of an individual AgPS from group A020 as function of time.
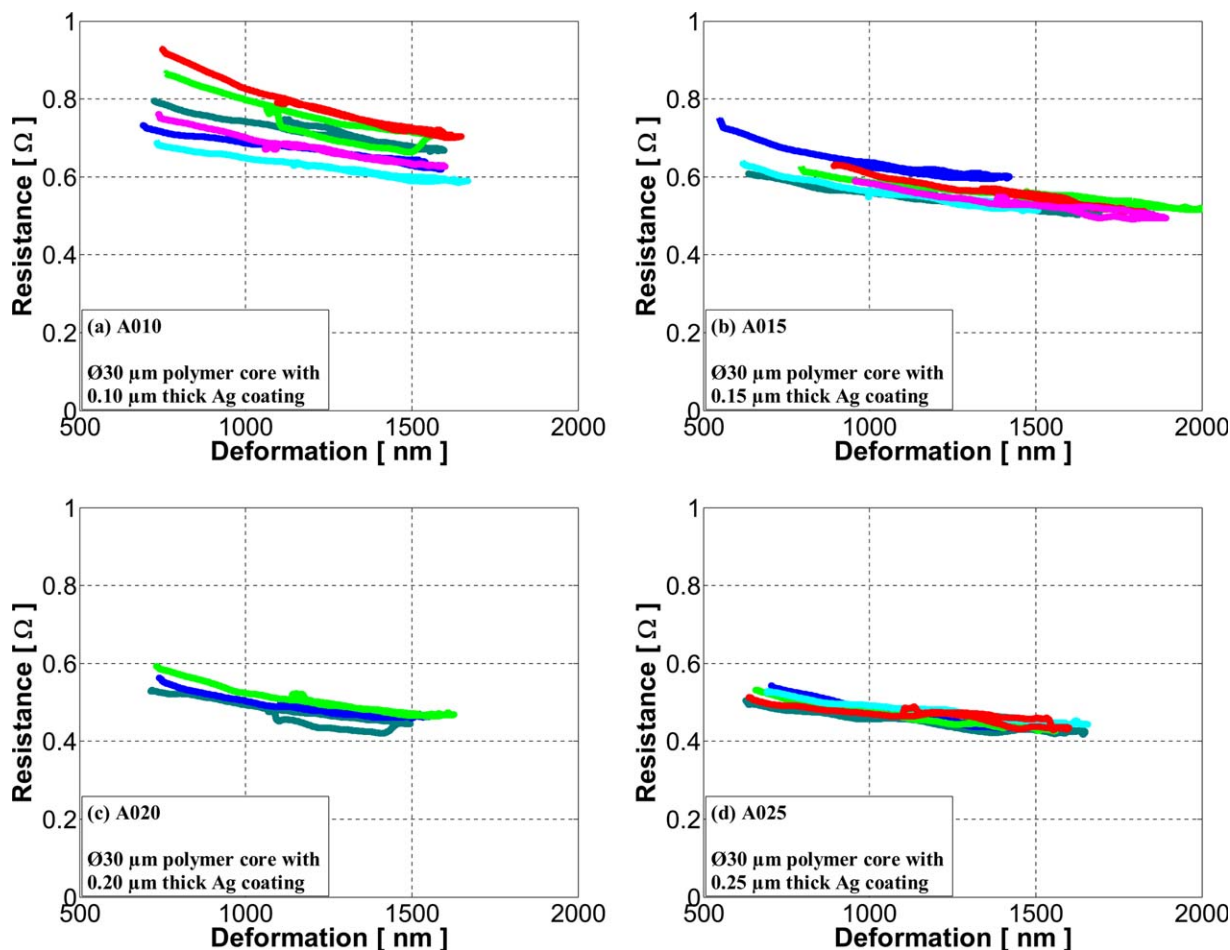
Figure 6. Measured resistance-deformation curves for the four groups of AgPS. Each curve in a graph presents measurement result of an individual particle from the corresponding group. [Color figure can be viewed in the online issue, which is available at wileyonlinelibrary.com.]

interconnects based on anisotropic conductive adhesives (ACAs).[20,23–25] These two models were found to be applicable even though their inherent assumptions might not be totally accurate for ACA interconnects.[23–25] Our experimental setup to characterize individual AgPS [Figure 2(a)] was similar to an ACA interconnect. In addition, the deformation degree of tested AgPS was small (about 6%). Hence, Holm's and Hertz's models [eqs. (1) and (2)] were employed to estimate the constriction resistance between AgPS particles and the flat punch, and that between particles and the Au-coated substrate. The total interfacial contact resistance is then estimated by using the following equation.

$$R_{IC} = \left(\frac{\rho_{WC\text{-}Co} + \rho_{Ag}}{4 \cdot a} \right) + \left(\frac{\rho_{Au} + \rho_{Ag}}{4 \cdot a} \right) \quad (3)$$

where R_{IC} is the total interfacial contact resistance between particles and the surfaces of the flat punch and the Au-coated substrate; $\rho_{WC\text{-}Co}$, ρ_{Au} and ρ_{Ag} are the electrical resistivity of the WC-Co punch, the Au-coated substrate and the Ag coating, respectively; and a is the contact radius estimated from eq. (2). Using the resistivity values of WC-Co (200 nΩ·m),[17] pure Au (22.7 nΩ·m at 25 °C) and pure Ag (15.9 nΩ·m at 25 °C)[26] in eqs. (2) and (3), R_{IC} was estimated as shown in Figure 8. At the same deformation degree of a particle, the estimated R_{IC} is rela-

tively small compared to the measured resistance of the particle. For comparison purpose, the estimated R_{IC} was scaled up to the same range as the measured data for each group of AgPS. The
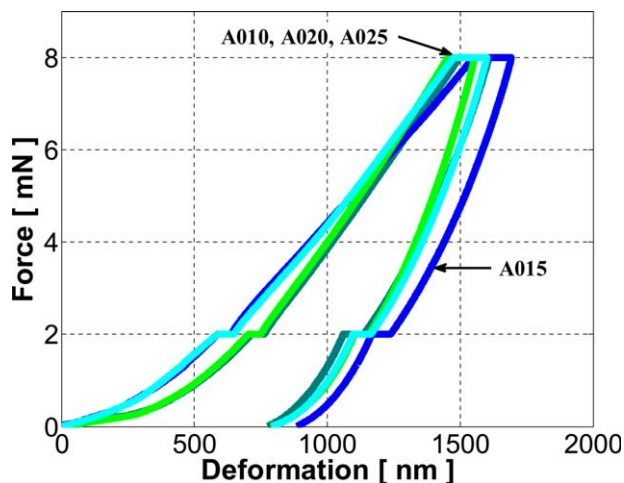

Figure 7. Comparison of mechanical response for the four groups of AgPS tested. The force-deformation curve corresponding to each group of particles is represented by the median curve (see Figure 3). [Color figure can be viewed in the online issue, which is available at wileyonlinelibrary.com.]
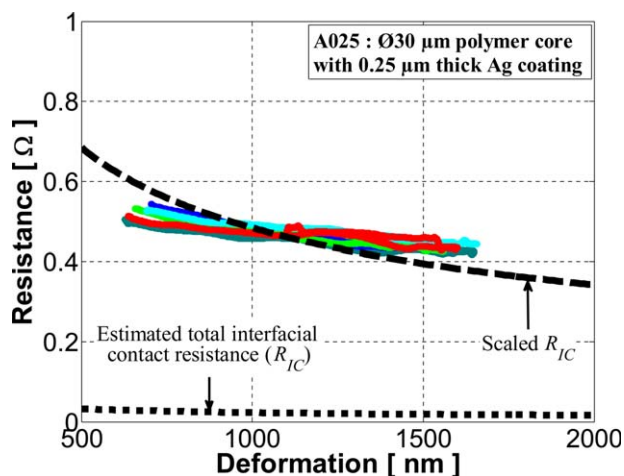
Figure 8. Comparison between total interfacial contact resistance and measured resistances of individual particles as function of particle deformation. Results of A025 particles are selected as an example and shown as solid lines in the figure. The dotted line corresponds to the total interfacial contact resistance (R_{IC}) estimated using eqs. (2) and (3). The dashed line corresponds to R_{IC} being scaled up to the same range as the measured data. [Color figure can be viewed in the online issue, which is available at wileyonlinelibrary.com.]

physical meaning of R_{IC} being scaled up is that the effective contact radius (i.e., contact area) is smaller and proportional to the nominal contact radius estimated using eq. (2). Scaling of R_{IC} can also be interpreted as higher effective resistivity of the WC-Co punch as well as the Au and the Ag coatings, compared to theoretical values of the pure materials. For the four groups of AgPS tested, the curves corresponding to scaled R_{IC} do not fit the experimentally observed resistance-deformation curves for individual particles. Figure 8 shows an example for A025 particles. The discrepancy between the R_{IC}–deformation curves and the experimentally observed resistance-deformation curves for individual particles indicates that the interfacial contact resistances are probably not the dominating factor in our measured data.

The estimation of the constriction resistances using Holm's and Hertz's models [eqs. (1) and (2)] is based on an assumption of perfectly smooth contact surfaces. In practice, the surfaces of the flat punch, the Au-coated substrate, and particularly the AgPS are rather rough with a number of asperities. That means the effective contact areas between the AgPS and the surfaces of the punch as well as the Au-coated substrate are probably much smaller than the nominal values estimated using eq. (2). Thereby, the effective constriction resistances are much higher than the "ideal" constriction resistances based on smooth contact surfaces. In a previous simulation study, Chen et al.[27] analysed effects of the roughness of contact surfaces on the constriction resistances of ACA interconnects with Au-coated polymer spheres. The effective constriction resistance was confirmed higher than the "ideal" one based on smooth contact surfaces. Their results also indicated that the difference between the effective and the "ideal" constriction resistance was large at small deformations and decreased with increasing deformation

of asperities. At a certain deformation degree of asperities, the effective constriction resistance was close to the "ideal" value for perfectly smooth surfaces. One should note that the deformation of asperities is according to the deformation of contacting bodies (e.g., particles), and that the constriction resistances are the main contributing factor for the interfacial contact resistances in our test setup. Hence, if we consider the roughness of contact surfaces, the new curve corresponding to the total interfacial contact resistance even has a steeper negative slope at small deformation degrees of AgPS, compared to the curves estimated based on perfectly smooth contact surfaces shown in Figure 8. The new curve with surface roughness considered is therefore not able to fit the measured resistance-deformation curves for individual AgPS.

As discussed above, the curves corresponding to the total interfacial contact resistance vs. deformation do not fit the experimentally observed resistance-deformation curves of individual AgPS, regardless of the surface roughness of the particles, the flat punch and the Au-coated substrate. This indicates that the interfacial contact resistances are not the dominating factor in our measured data.

Measurement results vs. Theoretical Model for Bulk Resistance of Individual AgPS. The resistance measurement results of the four groups of AgPS were compared with a theoretical model of Määttänen,[28] which was developed to predict the bulk resistance of an individual MPS. The Määttänen model was derived based on the geometry of a MPS under deformation. In addition, it was assumed that the area of the metal coating remains constant during the deformation. The formula of the Määttänen model is given in the following equation.

$$R_P = \frac{1}{\pi} \cdot \left(\frac{\rho}{t}\right) \cdot \ln \tan\left[\frac{\pi}{4} \cdot \left(1 + \frac{h}{\varnothing}\right)\right] = \frac{1}{\pi} \cdot \left(\frac{\rho}{t}\right)$$
$$\cdot \ln \tan\left[\frac{\pi}{4} \cdot \left(2 - \frac{D}{\varnothing}\right)\right] \tag{4}$$

where R_P is the bulk resistance of an individual MPS; ρ and t are the electrical resistivity and the thickness of the metal coating of the MPS, respectively; $\varnothing$ is the original diameter of the MPS; h is the distance between the two parallel surfaces in contact with the MPS [e.g., the flat punch and the Au-coated substrate in Figure 2(a)]; and D is the total deformation of the MPS ($D = \varnothing - h$). Using the electrical resistivity value for pure Ag (15.9 n$\Omega \cdot$m at 25 °C[26]) and the specified coating thickness, the Määttänen model underestimates our measurement results. At the same deformation degree of a particle, the predicted resistance is considerably lower than the measured value, as shown in Figure 9.

The higher measured resistances of individual AgPS, compared to the predicted values, could stem from several factors; (1) the contribution of the flat punch resistance as well as the interfacial contact resistances between the particles and the surfaces of the punch and the substrate; and (2) the physical properties of the Ag coating such as thickness and electrical resistivity. The contribution of the punch resistance and the interfacial contact resistances has been discussed in the previous section. In this section, we address two possible effects from the physical
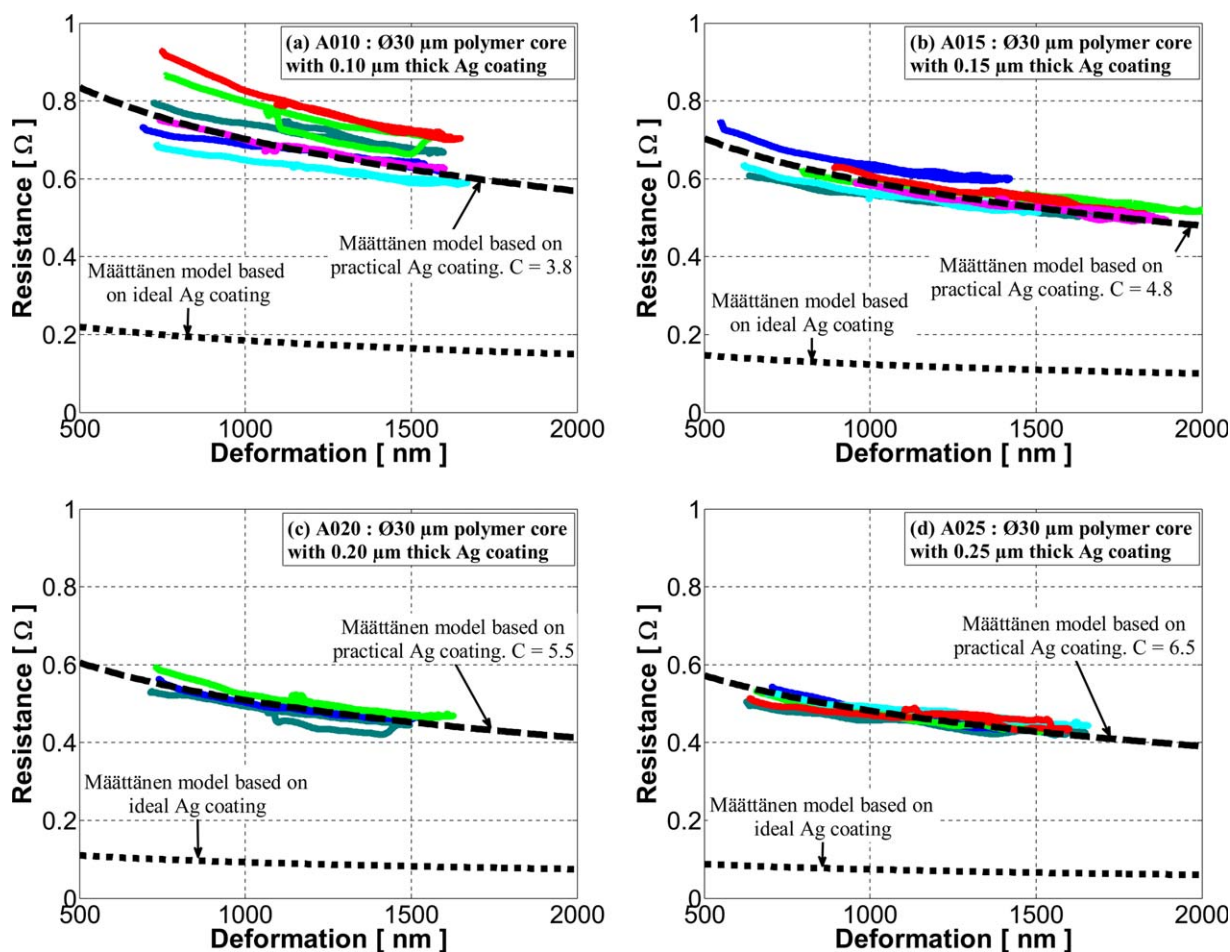
Figure 9. Comparison between experimental results and theoretical models for the four groups of AgPS. In each graph, the solid lines correspond to the measured resistance-deformation curves of individual particles shown in Figure 6; the dotted line corresponds to the Määttänen model based on ideal Ag coating [eq. (4)]; and the dashed line corresponds to the Määttänen model based on practical Ag coating with parameter *C* specified in eq. (5). [Color figure can be viewed in the online issue, which is available at wileyonlinelibrary.com.]

properties of the Ag coating; (i) the distribution and deviation of the coating thickness; and (ii) the effective resistivity of the Ag coating (compared to the resistivity of pure Ag). For a certain plating process, the effective coating thickness may have a deviation and a distribution from the objective thickness. In case the effective thickness of the Ag coating is smaller than the specified value, the measured resistances for individual particles are higher than the predicted values, which are based on the specified thickness. The effective resistivity of the Ag coating can be different from that of pure, smooth and uniform Ag layer, which was used to predict the particle resistances. Due to the plating process, the properties of Ag on the coating layer may be slightly changed compared to pure Ag. In addition, the Ag coating can also have imperfectness, such as Ag oxide and pores (see Figure 1). Therefore, the Ag coating can have a higher effective electrical resistivity than that of pure Ag, resulting in higher measured resistances than predicted values.

Taking into account the effective thickness and the effective resistivity of the Ag coating, the Määttänen model for the bulk resistance of an individual AgPS can be presented as followed.

$$R_p = \frac{1}{\pi} \cdot \left(\frac{\rho^*}{t^*} \right) \cdot \ln \tan \left[\frac{\pi}{4} \cdot \left(2 - \frac{D}{\emptyset} \right) \right] = \frac{1}{\pi} \cdot \left(C \cdot \frac{\rho}{t} \right)$$
$$\cdot \ln \tan \left[\frac{\pi}{4} \cdot \left(2 - \frac{D}{\emptyset} \right) \right] \tag{5}$$

where ρ^* and ρ are the effective and the ideal resistivity of the Ag coating, respectively; t^* and t are the effective and the ideally specified Ag coating thickness, respectively; C is a parameter corresponding to possible deviations of the effective thickness and the effective resistivity of the Ag coating from the ideally specified values; and D and $\emptyset$ are the total deformation and the original diameter of the particle, respectively. Figure 9 shows the comparison between the measured resistances of individual AgPS and the predicted resistances using the Määttänen model based on practical Ag coating. With an appropriate value of C for each type of AgPS, the Määttänen model fits the measured data reasonably well. This confirms our hypothesis of thinner effective coating thickness and/or higher effective resistivity of the Ag coating compared to the ideally specified values.

The measured data of an individual AgPS mainly include the bulk resistance of the particle and the interfacial contact

resistances between the particle and the surfaces of the flat punch and the Au-coated substrate. With appropriate values for the effective resistivity and the effective thickness of the Ag coating, the Määttänen model for the bulk resistance of individual particles reasonably fits the experimentally observed resistance-deformation curves. On the other hand, the commonly used models for estimating the total interfacial contact resistance (with and without roughness of contact surfaces considered) do not fit the measured resistance-deformation curves of individual particles. This indicates that the particle resistance dominates the measurement result of an individual AgPS in our experiments. Hence, the measured data in our study are claimed to represent the bulk resistances for individual AgPS.

CONCLUSIONS

The electrical resistance and the mechanical behavior of individual Ag-coated monodisperse polymer spheres (AgPS) were experimentally characterized using a nanoindentation-based flat punch method. Four groups of AgPS were tested. All tested particles have an identical polymer core (Ø30 μm) coated with an Ag layer of different thickness. The following conclusions can be drawn from the results and interpretations.

With a maximum loading force of 8 mN, the maximum deformation of particles is around 1.5–2 μm, corresponding to 5–7% of the particle diameter ($\sim$30 μm). At such low deformation degrees, the difference in mechanical response of AgPS with varying coating thickness (less than 2% of the polymer core radius) is small.

For the four groups of AgPS tested, the thicker the Ag coating is, the lower and more stable the measured resistance is. Particles with an Ag coating thickness of 0.25 μm exhibit good properties, in terms of repeatable mechanical response, as well as low and stable electrical resistance.

The experimental results showed that the electrical resistance of individual AgPS is dependent on the physical properties of the Ag coating such as thickness, uniformity, and porosity; the latter changes the effective electrical resistivity of the coating. This observation is supported by rather good agreement between the experimental results of the four groups of AgPS and a theoretical model for bulk resistance of individual particles, in which possible deviations of the effective resistivity and the effective thickness of the Ag coating from the ideally specified values are considered. Modeling the contact resistance between AgPS and the flat contacting pads shows that this contributes far less than the electrical resistance of the actual Ag-coated spheres. The measured data in the present work are thus claimed to represent the bulk resistances for individual AgPS.

The results from this characterization work for individual AgPS are a useful input for the development of a theoretical model that can predict the electrical resistance in macroscopic scale of isotropic conductive adhesives filled with Ag-coated polymer spheres.

ACKNOWLEDGMENTS

REFERENCES

1. Morris, J. E.; Liu, J. In Micro- and Opto-Electronic Materials and Structures: Physics, Mechanics, Design, Reliability, Packaging. Suhir, E.; Lee, Y. C.; Wong, C. P., Eds.; Springer Science+Business Media, Inc., **2007**; Vol. *2*; pp 527–570.

2. William, J.; Callister, D. In Fundamentals of Materials Science and Engineering, 5th ed.; Wiley, **2001**; pp 441–468.

3. Morris, J. E. *Microelectron. Reliab.* **2007**, *47*, 328.

4. Kristiansen, H.; Redford, K.; Helland, T. U.S. Pat. **2012**.

5. Kristiansen, H.; Redford, K.; Helland, T. U. K. Pat. **2012**.

6. Mundlein, M.; Nicolics, J. *IEEE Trans. Compon. Packaging Technol.* **2005**, *28*, 765.

7. Nguyen, H. V.; Andreassen, E.; Kristiansen, H.; Johannessen, R.; Hoivik, N.; Aasmundtveit, K. E. *Mater. Des.* **2013**, *46*, 784.

8. Nguyen, H. V.; Andreassen, E.; Kristiansen, H.; Aasmundtveit, K. E. *IEEE Trans. Compon. Packaging Manuf. Technol.* **2013**, *3*, 1084.

9. Nguyen, H.-V; Kristiansen, H.; Johannessen, R.; Andreassen, E.; Larsson, A.; Hoivik, N.; Aasmundtveit, K. E. In 61st Electronic Components and Technology Conference; Lake Buena Vista: Florida, **2011**; pp 639–644.

10. Jain, S.; Whalley, D. C.; Cottrill, M.; Kristiansen, H.; Redford, K.; Nilsen, C. B.; Helland, T.; Liu, C. In 18th European Microelectronics and Packaging Conference; Brighton, United Kingdom, **2011**; pp 1–7.

11. Jain, S.; Whalley, D. C.; Cottrill, M.; Helland, T.; Kristiansen, H.; Redford, K.; Liu, C. In 63rd Electronic Components and Technology Conference, Las Vegas, Nevada, **2013**; pp 796–802.

12. Dou, G.; Whalley, D.; Liu, C. In International Conference on Electronic Materials and Packaging (EMAP); Hongkong, China, **2006**; pp 1–9.

13. He, J. Y.; Zhang, Z. L.; Midttun, M.; Fonnum, G.; Modahl, G. I.; Kristiansen, H.; Redford, K. *Polymer* **2008**, *49*, 3993.

14. He, J. Y.; Zhang, Z. L.; Kristiansen, H. *J. Appl. Polym. Sci.* **2009**, *113*, 1398.

15. He, J. Y.; Helland, T.; Zhang, Z. L.; Kristiansen, H. *J. Phys. D Appl. Phys.* **2009**, *42*.

16. Helland, T. Master Thesis, Department of Materials Science and Engineering, Norwegian University of Science and Technology (NTNU), Trondheim, Norway, **2008**.

17. Properties of Tungsten Carbide from Manufacturers. Available at http://www.wesltd.com/divisions/hardmetal/html/Tungsten-carbide.html. http://www.tungstenchina.com/product/Tungsten-Carbide-Products.html http://www.rgpballs.

com/en/products/balls/metal-alloys/Tungsten-Carbide/Tungsten-Carbide-WC-with-Co-Binder-Alloys.

18. Holm, R. Electric Contacts: Theory and Application, 4th ed.; Springer-Verlag: Berlin, Germany, **1967**.

19. Zhang, P.; Lau, Y. Y.; Tang, W.; Gomez, M. R.; French, D. M.; Zier, J. C.; Gilgenbach, R. M. In 57th Holm Conference on Electrical Contacts (Holm); Minneapolis, 2011; pp 1–6.

20. Chin, M.; Iyer, K. A.; Hu, S. J. *IEEE Trans. Compon. Packaging Technol.* **2004**, *27*, 317.

21. Johnson, K. L. Contact Mechanics; Cambridge University Press, **1987**.

22. Liu, K. K.; Williams, D. R.; Briscoe, B. J. *J. Phys. D Appl. Phys.* **1998**, *31*, 294.

23. Kwon, W. S.; Paik, K. W. *IEEE Trans. Compon. Packaging Technol.* **2006**, *29*, 528.

24. Yim, M. J.; Paik, K. W. *IEEE Trans. Compon. Packaging Manuf. Technol. A* **1998**, *21*, 226.

25. Lu, S. T.; Chu, H. M.; Chen, W. H. *IEEE Trans. Dev. Mater. Reliab.* **2013**, *13*, 54.

26. Aylward, G. H.; Findlay, T. J. V. SI Chemical Data, 6th ed., Wiley, **2008**.

27. Chen, X.; Tao, B.; Yin, Z. In 12th International Conference on Electronic Packaging Technology and High Density Packaging; Shanghai, China, **2011**.

28. Määttänen, J. *Soldering Surf. Mount Technol.* **2003**, *15*, 12.

Ø30 μm Ag-coated polymer spheres